ADVANCED FUNCTIONAL MATERIALS
www.afm-journal.de

Fabricating Strong and Stiff Bioplastics from Whole Spirulina Cells

*Hareesh Iyer, Paul Grandgeorge, Andrew M. Jimenez, Ian R. Campbell, Mallory Parker, Michael Holden, Mathangi Venkatesh, Marissa Nelsen, Bichlien Nguyen, and Eleftheria Roumeli**

Since the 1950s, 8.3 billion tonnes (Bt) of virgin plastics have been produced, of which around 5 Bt have accumulated as waste in oceans and other natural environments, posing severe threats to entire ecosystems. The need for sustainable bio-based alternatives to traditional petroleum-derived plastics is evident. Bioplastics produced from unprocessed biological materials have thus far suffered from heterogeneous and non-cohesive morphologies, which lead to weak mechanical properties and lack of processability, hindering their industrial integration. Here, a fast, simple, and scalable process is presented to transform raw microalgae into a self-bonded, recyclable, and backyard-compostable bioplastic with attractive mechanical properties surpassing those of other biobased plastics such as thermoplastic starch. Upon hot-pressing, the abundant and photosynthetic algae spirulina forms cohesive bioplastics with flexural modulus and strength in the range 3–5 GPa and 25.5–57 MPa, respectively, depending on pre-processing conditions and the addition of nanofillers. The machinability of these bioplastics, along with self-extinguishing properties, make them promising candidates for consumer plastics. Mechanical recycling and fast biodegradation in soil are demonstrated as end-of-life options. Finally, the environmental impacts are discussed in terms of global warming potential, highlighting the benefits of using a carbon-negative feedstock such as spirulina to fabricate plastics.

1. Introduction

The worldwide consumption of petrochemical-based plastics has been increasing alarmingly for decades. The total amount of plastic produced by 2050 is predicted to be 33 billion tons, compared to 0.28 billion tons in 2012.[1] As a result of improper classification, sorting, and disposal strategies, plastic waste collects in landfills, waterways, and oceans, causing significant hazards to human health and the environment.[2–5]

The chemical stability of common plastics makes them attractive for numerous applications, but is also responsible for slow degradation rates, which allow them to permeate the environment before fully degrading.[6] During these long degradation timeframes, plastics are fragmented into smaller pieces, termed microplastics, that can seep into food and water systems at all levels of the food chain, causing health hazards throughout the environment.[5,7] Even when properly disposed of, commodity plastics are most often incinerated, releasing carbon dioxide (CO_2) into the environment.[3] The combustion of petrochemical plastics rapidly transfers carbon from the slow (thousands of years) to fast (human lifetimes) carbon cycle.[8] To comply with the Conference of Parties agreement from 2015 (COP21) and limit the rise of global temperatures to 1.5 °C compared to pre-industrial levels, new materials must be developed with less harmful effects on the environment.

Petrochemically-derived, biodegradable polymers such as polybutylene adipate terephthalate (PBAT), and biologically-derived (biobased), non-degradable polymers such as bio-polyethylene, have been developed as more sustainable alternatives to commodity plastics. However, either the petrochemical origin or the inability to degrade limit the suitability of such materials to meet sustainability goals. Biobased and biodegradable polymers, such as the widely available polylactic acid (PLA) and poly(hydroxyalkanoate)s (PHAs), have the potential to reduce petroleum dependency and plastic pollution.

PLA, the largest production volume alternative, can only be composted in specific environmental conditions for which industrial facilities are required, but such facilities may not be easily accessible in communities around the world.[9] Promising lab-scale results have demonstrated the use of aliphatic polyesters and silyl ethers derived from biomass as a versatile platform to design copolymers that are biobased and can biodegrade in mild conditions.[4,10–12] Similarly, PHAs can be extracted from

H. Iyer, P. Grandgeorge, A. M. Jimenez, I. R. Campbell, M. Parker, M. Holden, M. Venkatesh, M. Nelsen, E. Roumeli
Materials Science and Engineering
University of Washington
302 Roberts Hall, Seattle, WA 98195, USA
E-mail: eroumeli@uw.edu
B. Nguyen
Microsoft Corporation
1 Microsoft Way, Redmond, WA 98052, USA

The ORCID identification number(s) for the author(s) of this article can be found under https://doi.org/10.1002/adfm.202302067

DOI: 10.1002/adfm.202302067

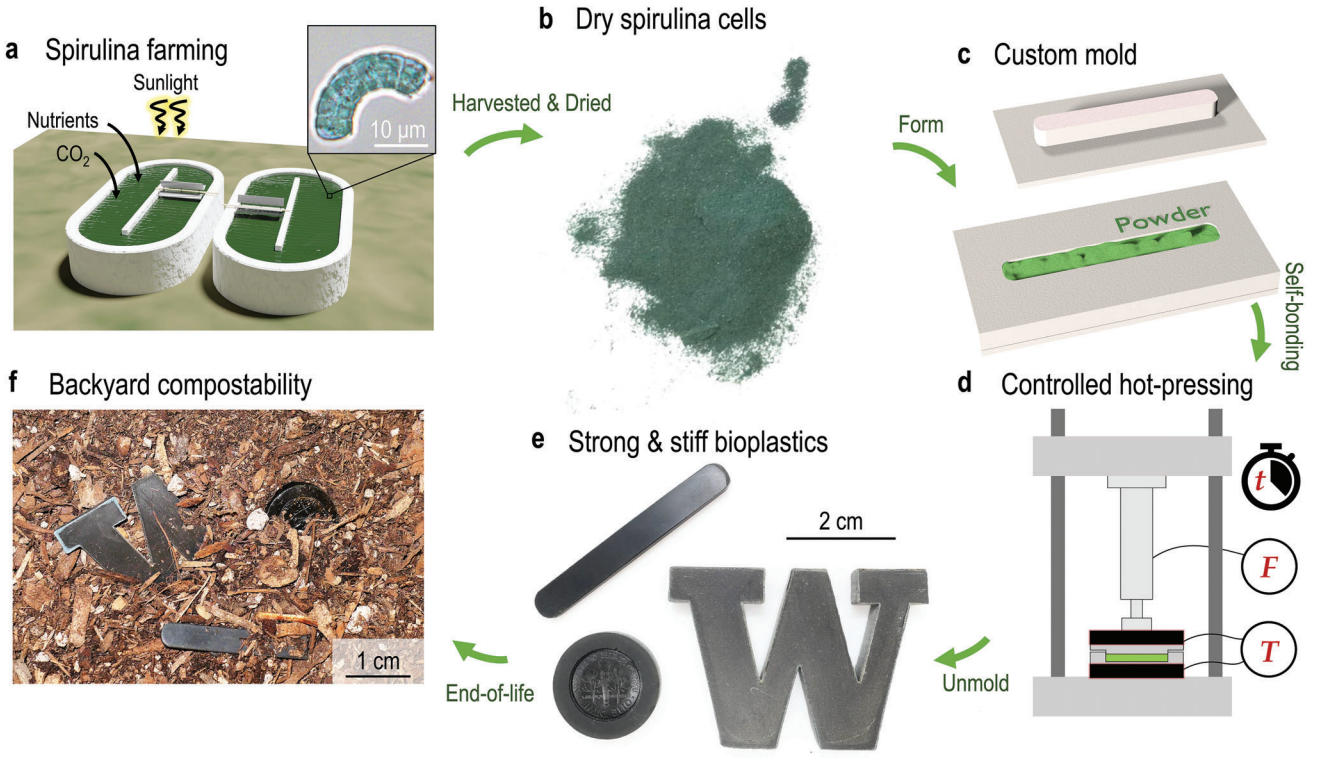

Figure 1. From spirulina to biodegradable bioplastics. a) Spirulina cells are cultivated at scale for commercial applications. b) Commercial spirulina powder used in this study. c) Conventional manufacturing techniques such as compression molding in a hot-press can be used to turn spirulina cells into d) bioplastics that are e) backyard compostable in soil.

biomass feedstocks, food waste, or microbial cultures, and the resulting polyesters have been used in generating over 150 different copolymers.[6,13–16] Still, scalability challenges and economic feasibility limit the range of applications of PHAs.[16,17]

Another route to creating sustainable plastics is utilizing thermoplastic starch (TPS) from abundant feedstocks such as maize, wheat, potato, rice, etc.[18,19] Most commonly, starch extracted from biomass is treated with heat and pressure in the presence of water to disrupt the order within the amylose and amylopectin macromolecular chains. Plasticizers such as glycerol or others polyols are then mixed in to allow thermoformability in the resulting TPS.[20] The applications of TPS are limited by its relatively low strength of less than 6 MPa.[18,19] Lignocellulosic polymers can provide a biobased source for materials with higher strength and stiffness values due to the inherent high degree of crystallinity and strength of cellulose,[1,18,21–24] and can be considered carbon sinks when made from waste biomass that would otherwise be incinerated. Still, the extraction of cellulose from biomass involves multi-step processes and harsh chemicals.[25,26] Interestingly, macro- and microalgae (e.g., spirulina or chlorella species), owing to their wide availability and the capability to be cultured on non-arable lands, have been used as natural organisms to extract PHA[14,15] and cellulose,[27] and some have been genetically engineered to enhance starch biosynthesis.[28]

In an effort to circumvent extraction processes, biobased and compostable materials produced from *whole* plant, bacterial, fungal, or algal biomass, without extracting components, have been reported.[1,24,29–36] Among the studied organisms, algal species can be considered as a potentially disruptive material platform as they grow rapidly in a wide variety of natural aquatic environments as well as in cultures.[28,30] This versatility may allow for algae to be grown in close proximity to facilities where they are transformed into bioplastic materials, reducing transportation emissions and costs. In addition, photosynthetic algae act as a carbon sink, thereby reducing the quantity of global atmospheric carbon dioxide.

Prior work from Zeller et al.[36] focused on using unmodified *Arthrospira platensis* (spirulina) and *Chlorella vulgaris* (chlorella) cells to form bioplastics by subjecting them to heated compression molding. That work demonstrated thermoformability, but the produced bioplastics showed poor tensile strengths of 5.7 and 3.0 MPa, respectively. Fredricks et al.[30] demonstrated that unmodified spirulina cells can also be used in additive manufacturing to create inks for direct ink writing. The printed structures had mechanical properties and micromorphologies dependent on the drying method. The limited understanding of mechanisms to precisely transform algal biomass to bioplastics, as well as the poor mechanical properties that have been presented in prior literature, hinder the application of this material class, especially as a replacement for high-volume commodity plastics.

Here, we present a fast and scalable method to produce strong and stiff backyard-compostable bioplastics from spirulina cells, without the use of any binders or additives, by subjecting them to conventional heated compression molding (procedure outlined in **Figure 1**). Starting from raw spirulina, an abundant and commercially available microalgal species (Figure 1a,b), we followed

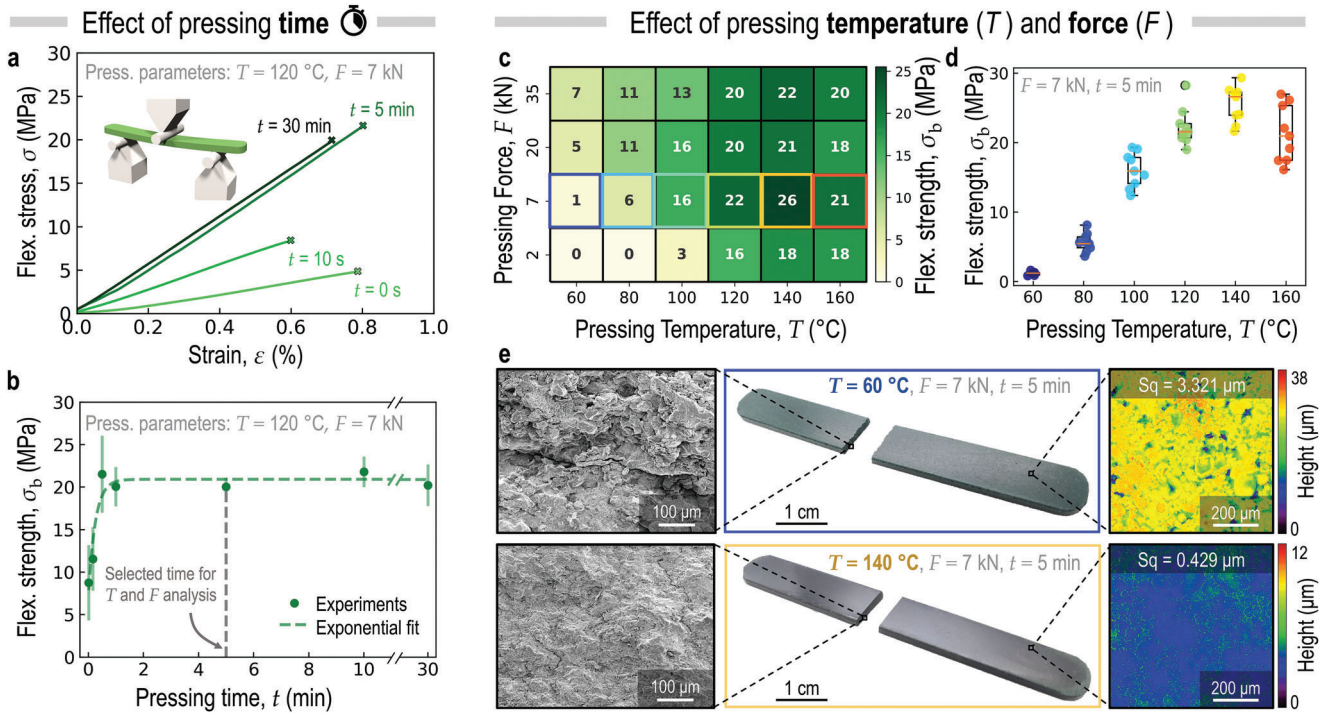

Figure 2. Mechanical and morphological properties of pure spirulina bioplastics. a) Representative stress-strain curves for spirulina at different pressing times. b) Flexural strength of spirulina bioplastics with varying pressing times. c) Heat map of flexural strength for spirulina bioplastics at each temperature/pressure range. d) Flexural strength versus pressing temperature for a fixed pressing force (7kN; corresponding to a pressure of 14.9 MPa) and time (5min). e) Scanning electron microscopy (SEM) images (left) and optical profilometry (right) of the weakest spirulina sample (top line), compared to the best spirulina sample (bottom line).

a manufacturing process that enables the utilization of the entire microorganism without extraction or chemical modification processes. Upon the application of heat and pressure at optimal conditions (Figure 1c), the spirulina powder bonds into a rigid, thermoformable bioplastic that can be further processed and machined like a thermoplastic. We assessed the mechanical properties of our bioplastics by performing flexural tests on hot-pressed beams. By systematically varying the pressing time, temperature, and pressure (Figure 1d), we modulated the mechanical properties of the obtained bioplastics by controlling the micromorphology and bonding of the cell matrix. The optimized bioplastics reached strengths and moduli comparable or higher than those of commodity plastics and surpassed those of TPS and previously reported algal bioplastics, while being processable with existing polymer manufacturing infrastructure (Figure 1e), and being backyard compostable (Figure 1f).

2. Results

2.1. Pure Spirulina Bioplastics

To optimize the pressing conditions for the fabrication of strong, pure spirulina bioplastics, we first studied the effects of varying the processing conditions (pressing time, temperature, and force) on the resulting mechanical properties and morphology of spirulina bioplastics. First, we analyzed the effect of progressively varying the pressing time, t, between 0 and 1800 s (30 min) under fixed temperature and pressing force conditions of T = 120 °C and F = 7 kN (corresponding to an applied pressure of 14.9 MPa). We then conducted flexural tests on the resulting samples, for which representative stress-strain curves are presented in **Figure 2**a. Note that the pressing time was started once the desired pressing force was reached. The flexural strength (σ_b) is reported as a function of pressing time in Figure 2b, along with an exponential fit (dotted green line) of the form:

$$\sigma * (t) = \sigma_0 + (\sigma_p - \sigma_0)\left(1 - \exp^{-t/\tau}\right) \quad (1)$$

According to this fit, the strength increases from $\sigma_{t=0}$ = 8.8 MPa up to a plateau value of approximately σ_p = 20.9 MPa with a characteristic time constant τ = 15.4 s. At pressing times below 60 s ($\approx 4\tau$), the strength is significantly lower than the plateau strength and the data exhibit higher standard deviations than at longer pressing times. Below this threshold, the pressing time is not sufficient to facilitate the formation of a bonded uniform spirulina matrix. This lack of self-bonding may either be caused by insufficient time for the mold and spirulina to reach the set temperature or because the necessary reactions leading to self-bonding require more thermal energy input and time to complete.

Next, we investigated the effects of pressing temperature and force on the mechanical properties of the bioplastics formed. For each value of T and F, the pressing time was fixed to the conservative value of 300 s (20τ, dotted line in Figure 2b), to ensure that the strength plateau could be reached and to accommodate for lower pressing temperatures and forces than the ones used in the

time-variant experiment. At that fixed pressing time, we varied the temperature from 60 to 160 °C and the pressing force from 2 to 35 kN (corresponding to applied pressures in the range from 4.3 to 74.5 MPa, see Table S1 in the Supporting Information for force to pressure conversions). In Figure 2c, we present a heat-map of the measured flexural strength values for each of the tested temperature-pressure conditions. A region of maximal strength is observed for temperatures between 120 and 160 °C and a pressing force of 7 kN. Figure 2d shows the relationship between flexural strength and pressing temperature at a force of 7 kN. We observe a progressive strength increase with increasing temperature up to a maximum value at 140 °C, beyond which strength decreases. This drop in strength at high temperatures (160° C), is seen for all pressing forces at or above 7 kN and can be attributed to the initiation of thermal degradation reactions in spirulina. Indeed, the thermal degradation profile of spirulina (presented in Figure S1, Supporting Information) shows that degradation starts at around 180 °C. The bending modulus and toughness follow similar trends as the strength (Figure S2, Supporting Information). Overall, our mechanical tests show a strong dependency of the flexural strength of the produced bioplastics on the pressing temperature, with variations between the weakest bioplastic pressed at 60 and strongest at 140 °C (both pressed at $F = 7$ kN; pressure of 14.9 MPa) as high as 2080%. We further characterized the compressive mechanical properties of the optimally-pressed spirulina bioplastics. Interestingly, compression tests (Figure S3, Supporting Information) reveal a nearly isotropic behavior. Compressive strength was measured at 76.1 ± 3.9 MPa in the axial direction (with respect to the hot-pressing direction), and 70.2 ± 2.9 MPa in the transverse direction (7.7% difference). We attribute this small but statistically significant difference (p-value 0.04) to the fact that during the fabrication process, the compaction and binding of the bioplastics are naturally enhanced along the hot-pressing direction before a continuous matrix is formed.

Scanning electron microscopy (SEM) images of the fracture surfaces of the weakest and strongest bioplastics are presented in Figure 2e. From these images, we observe that the bioplastics pressed at 60 °C consist of compacted cells which have not formed a uniformly bonded matrix, unlike the homogeneous surface of the samples pressed at 140 °C. Therefore, we propose that increasing the pressing temperature enables the transition from a loosely bonded mass of cells to an amorphous uniform matrix in which cell outlines can no longer be observed. Energy dispersive X-ray spectroscopy (EDS) spectra, presented in Figure S4 (Supporting Information), show that nitrogen is evenly dispersed throughout the matrix of the bioplastic. This indicates that there is no phase separation or aggregation of protein, the dominant component by weight in our spirulina. The morphological uniformity ultimately endows the bioplastic with the remarkable stiffness and strength measured here. Optical profilometry tests on the bioplastics pressed at 60 versus 140 °C (Figure 2e), corroborate the microscopic observations and show that the well-bonded sample has a smoother surface with a root mean square height $S_q = 430$ nm, while for the poorly bonded sample, $S_q = 3.3$ µm. The profilometry maps also reveal the cell outlines on the surface of the weakest sample, in agreement with the SEM observations, while no cell outlines are seen on the strongest sample. The smoothness of the strongest bioplastics is advantageous when producing faithful imprints of fine details through the use of positive molds, as demonstrated in Figure 1e. The roughness of the fracture surface of the weakest and strongest samples was also assessed using optical profilometry (presented in Figure S5, Supporting Information). As expected, the well-bonded bioplastic resulted in a smoother surface ($S_q = 3.214$ µm) than the weakly-bonded samples ($S_q = 8.978$ µm). The mean square height of the weakly-bonded fracture surface is on the order of the spirulina cell dimensions, revealing once more that this sample corresponds to a compacted powder, whereas the well-bonded conditions enable the cells to fuse together.

Our mechanical and morphological results collectively suggest that in a pure spirulina system, the gradual transition from compacted intact cells to a fully-bonded matrix of dissociated cells, achieved through increasing the pressing temperature above a threshold for a given combination of pressing force and time, leads to the progressive increase in the measured mechanical properties of our bioplastics. The attainable range resulting from modulating the pressing conditions is 1.2–25.5 MPa for flexural strength, 0.35–3.1 GPa for flexural modulus, 0.63%–1.14% for strain to break, and 0.01–0.14 MJ m^{-3} for work to fracture, highlighting that the resulting bioplastics can compete in terms of performance with state-of-the-art commodity bioplastics. For comparison, PLA has a strength of 21–60 MPa and stiffness of 0.35–3.5 GPa,[37] TPS has a strength below 6 MPa and stiffness less than 1 GPa,[18,19] and previously reported spirulina bioplastics have a strength of 3.0 MPa and stiffness of 249 MPa[36]).

To further understand the changes in bonding that lead to the observable changes in the mechanical and morphological properties of our bioplastics, we conducted Fourier Transform Infrared (IR) spectroscopy and X-ray Photoelectron Spectroscopy (XPS) on the spirulina powder and weakest and strongest samples (pressed at 60 and 140 °C, respectively), presented in **Figure 3**. Complete spectra and assignment of the IR peaks can be found at (Figure S6 and Table S2, Supporting Information). The infrared spectra (Figure 3a) reveal significant differences between the spirulina powder and the bioplastic pressed at 140 °C. Thermomechanical processing at those conditions causes the Amide I, II, and III protein bands of spirulina to shift toward, and increase intensity at, lower wavenumbers. Most notably, the intensity of the Amide I band (1600–1700 cm^{-1}) of pressed spirulina increases significantly at 1623 cm^{-1}. The distinctive double peak formed in the strongest sample contrasts the broad Amide I band in spirulina powder centered at 1635 cm^{-1}. The Amide II and III bands also shift from 1539 to 1533 cm^{-1} and 1237 to 1230 cm^{-1}, respectively. Together, these transitions indicate the formation of β-sheet conformations in spirulina proteins during pressing.[38–40] These patent shifts observed in the Amide bands of spirulina pressed at 140 °C are not observed after pressing at 60 °C. While there is a lesser shift in the Amide III band (from 1237 to 1234 cm^{-1}), the shapes and locations of the Amide I and II bands remain unchanged after hot-pressing using more mild conditions. This suggests that the protein transformation experienced during processing at 140 °C does not occur for the pressing at 60 °C. β-sheet conformations are associated with higher strength and stiffness in proteins than α-helices.[41,42] Therefore, the IR observations of an increased amount of β-sheets in the protein-rich spirulina matrix upon thermomechanical processing at a higher

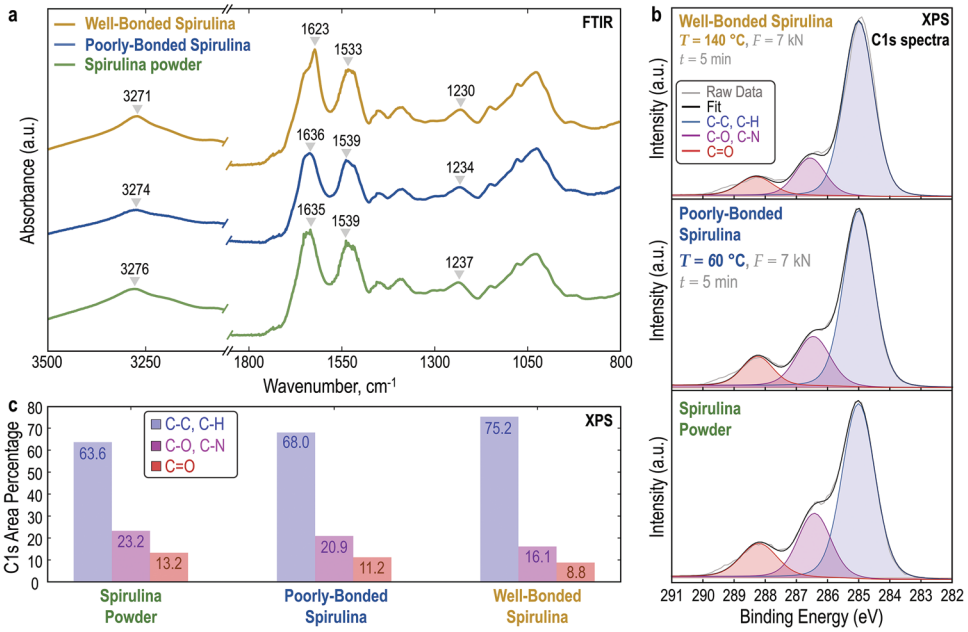

Figure 3. Bond analysis of pure spirulina bioplastics. a) Infrared spectroscopy of spirulina powder, poorly-bonded bioplastic (60 °C, 7 kN, 5 min), and well-bonded bioplastic (140 °C, 7 kN, 5 min). b) Area percentage numbers for the C–C/C–H, C–O/C–N, and C=O peaks as deconvoluted from the C1s spectra. c) C1s spectra from XPS for the spirulina powder, poorly-bonded bioplastic, and well-bonded bioplastic. Includes deconvoluted peaks corresponding to the C–C and C–H bonds, C–O and C–N bonds, and C=O bonds.

temperature (140 °C) support the improved mechanical properties compared to the sample pressed at 60 °C.

Additionally, the IR spectra reveal a redshift in the O–H band of spirulina (3276 cm^{-1}) after pressing at both 60 °C (3274 cm^{-1}) and 140 °C (3271 cm^{-1}). Shifts in the O–H peak indicate changes in hydrogen bonding.[43] The slight shift for the 60 °C pressed spirulina, for which significant protein conformational transformation does not occur, may indicate an increase in intermolecular hydrogen bonding that is unrelated to the formation of beta sheets. Therefore, this result suggests that the samples formed at the low-temperature condition are held together via intermolecular hydrogen bonding between the different biopolymers present in the spirulina cell walls and protoplasm, which are typically rich in surface hydroxyl groups.[44,45] Other types of intermolecular interactions such as biopolymer chain entanglement and Van der Waals interactions may also contribute to the bonding of the samples pressed at lower temperatures. The more significant redshift of the O–H bond in the absorption spectrum of the sample pressed at 140 °C indicates more intermolecular hydrogen bonding in that sample. In this case, increased intermolecular hydrogen bonding can be attributed to both enhanced hydrogen bonding between biopolymers in the spirulina and the transition from α-helices (intramolecular connections) to β-sheets (intermolecuar connections).

The deconvolution of the collected XPS spectra (Figure 3b,c) reveals further changes in the bonding motifs of our materials. We observe a significant decrease in the relative amount of C=O, C–O, and C–N bonds in the hot-pressed materials, in comparison to the unpressed powder. Specifically, compared to the raw spirulina powder, the weakest bioplastic has 15% fewer C=O and 10% fewer C–O/C–N bonds while the strongest bioplastic has 33% fewer C=O and 31% fewer C–O/C–N bonds. Both pressed samples have higher amounts of C–C/C–H groups compared to the unpressed powder (7 and 18% higher respectively for the 60 and 140 °C). The spirulina cells used in this study are comprised of 54.2–63.1% protein as measured by elemental analysis (CHN), 15% saccharidic carbohydrates and 15% acid-soluble phenolics as determined by high–performance liquid chromatography (HPLC),[30] 1.9–7.8% lipids,[46–48] and 1–10% PHA.[15,49] We first consider the dominant biopolymer components (proteins, glucose-based carbohydrates and phenolics)[30] to understand the possible changes in bonding. Proteins are rich in carbonyl groups in the peptide chains, some of which are exposed in the folds, turns, and chain ends of the proteins. Carbohydrates on the other hand are rich in pendant C–O groups. These groups are also present in the main sugar chain but the side groups are more reactive.[50] Aromatic compounds in spirulina also offer a variety of functional groups including C=O and C–O pendant groups.[45,50] We hypothesize that heat and pressure facilitate reactions of the C=O and C–O bonds at chain ends and pendant sites which result in the increased amount of C–C bonds measured in the spectra of hot-pressed samples. Therefore, we observe distinct changes in the covalent bond makeup of the spirulina samples upon hot pressing in addition to the hydrogen bonding suggested by the IR spectra. Our data collectively suggest that the processing of spirulina powder with heat and pressure leads to changes in covalent bonding and enhances the secondary interactions between the biopolymers within the biomatter in addition to causing conformational changes (β-sheet formation) in the protein matrix. These changes together support the measured increases in the mechanical properties as the biomatter is processed at higher temperatures. The presence of PHA in spirulina may also contribute to the bonding of the bioplastics, but because of its relatively low concentration[15,49]

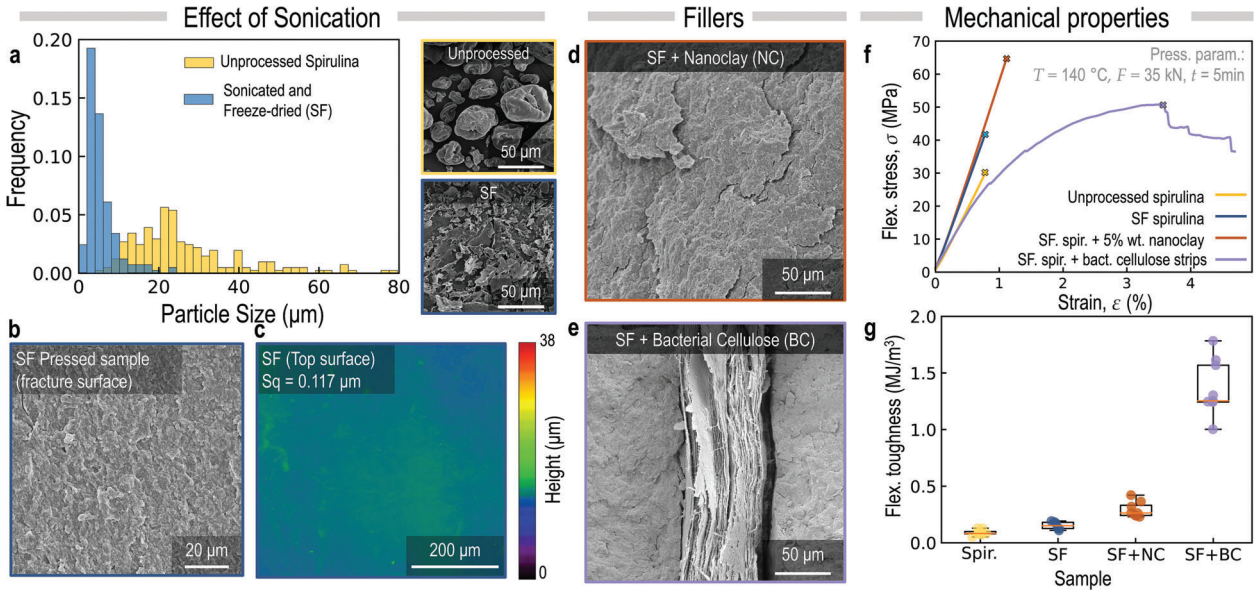

Figure 4. Sonication and reinforcement fillers in spirulina. a) Particle size distribution of unprocessed and sonicated (SF) spirulina cells and corresponding SEM images. b) SEM and c) optical profilometry images of the spirulina bioplastics created from sonicated cells. SEM images of the fracture surfaces of bioplastic nanocomposites containing d) nanoclay (NC) and e) bacterial cellulose (BC). f) Comparison of representative stress-strain curves of pure spirulina, sonicated spirulina, sonicated spirulina with NC, and sonicated spirulina with BC. g) Effects of sonication and fillers on the toughness of the generated bioplastics.

and high melting point,[14,51] its contributions are likely minimal compared to those of the other biopolymers discussed above.

2.2. Mechanical Property Tunability

To expand the mechanical property space of the spirulina bioplastics, we investigated mechanical pre-treatments of the cells, as well as introducing additives to form nanocomposites. First, we hypothesized that mechanically pre-treating the spirulina cells to dissociate them would improve bonding, as a higher surface area would be available for interactions during the pressing step. We sonicated the as-received cells in water (see Section 4), as ultrasonication has been proven to cause cell disruption in spirulina cells.[52,53] SEM images confirm that sonication leads to cell dissociation and, as a result, to a substantial particle size reduction from 28.3 ± 16.6 to 5.5 ± 3.5 μm (**Figure 4**a). Following this step, we freeze-dried and ground up the sonicated spirulina before pressing it at 140 °C, and 35 kN, for 5 min. The morphological analyses through SEM and optical profilometry reveal that the cell disruption via sonication further improves the homogeneity of the matrix after hot-pressing (Figure 4b,c) leading to the smoothest surface with $S_q = 117 \pm 60$ nm. Figure 4f shows representative three-point bend stress-strain curves of sonicated spirulina bioplastic compared to the non-sonicated equivalent (solid green and purple lines, respectively). On average, the sonicated spirulina has a bending strength of 35.1 ± 4.5 MPa, corresponding to a 38% increase compared to the strongest unprocessed spirulina sample, while the modulus is also increased by 58%. Therefore, mechanical pre-treatment alone can be an effective strategy to improve the attainable properties of pure spirulina bioplastics.

Next, in an attempt to further improve the mechanical properties of our bioplastics, we incorporated nanoclay platelets and bacterial cellulose (BC) sheets as nanofillers in the spirulina matrix. The incorporation of nanofillers is a common approach to enhance the mechanical properties of conventional polymers.[54,55] We selected nanoclay and BC as case studies because of their exceptional mechanical properties, hydrophilic nature, and compatibility with our biopolymer matrix, as well as for their distinctly different morphology and aspect ratios.[23,56] Specifically, the layered conformation and terminal oxygen planes in the tetrahedral structure of montmorillonite (MMT), our nanoclay of choice, would allow enhanced surface interactions and hydrogen bonding with the protein- and carbohydrate-based spirulina matrix.[30] We note that sonication of the nanoclay and spirulina in water are necessary to promote filler dispersion and enhance interactions by dissociating the cells. Indeed, upon freeze-drying and hot pressing the nanocomposite bioplastics, we observe that a 5 wt.% nanoclay concentration leads to an improvement of the average flexural strength from 35.1 ± 4.5 to 57.2 ± 7.4 MPa (63% increase), a increase in work to fracture from 0.15 ± 0.03 to 0.29 ± 0.06 MJ m^{-3} (93% increase), and an increase in stiffness from 3.9 ± 0.7 to 5.3 ± 0.3 GPa (36% increase) over sonicated and freeze-dried spirulina without the nanoclay (Figure 4f, solid blue line). SEM images of the nanoclay nanocomposites show no observable change in the micromorphology as compared to the neat sonicated spirulina (Figure 4d), suggesting sufficient dispersion of the nanoclay in the matrix. No visible aggregation was noted and bending failure occurred at the uniform matrix rather than in any filler-rich area. While further research will be necessary to thoroughly characterize the bonding between MMT and the matrix, the results show a significant increase in strength,

stiffness, and work to fracture at concentrations as low as 5 wt.% of MMT.

As a fiber nano-reinforcement for our spirulina matrix, we selected BC fibers due to their exceptional mechanical properties and high aspect ratio which, together with their abundant surface hydroxyl groups, would enable the formation of a strong network of interactions with the spirulina matrix biopolymers. In this example, we choose to use BC in the form of a sheet, as grown from a bacterial culture,[23] and create layered nanocomposites instead of isotropic ones. The ultra-long cellulose fibers synthesized by the cultured bacteria form a strong multilayered structure that utilizes the vast network of hydrogen bonding and physical interlocking of the intra- and inter-planar fibrils to achieve in-plane tensile strengths as high as 300 MPa and moduli up to 20 GPa.[57] As reported by Fredricks et al., the bacterial cellulose used in the present study had a tensile strength of ≈150 MPa and tensile modulus of ≈10 GPa.[23] Aiming to capitalize on the high strength and stiffness of the self-bonded cellulose sheets in their native (as-synthesized) state, we created a lamellar structure in which single layers of BC sheets were sandwiched between spirulina powder, before subjecting the composite to hot-pressing. The bending tests conducted in the plane normal to the BC sheets reveal that the addition of BC causes significant changes in the mechanical behavior of spirulina, as reflected in the representative stress–strain curve of Figure 4f (solid yellow line). While the stiffness of the composite is less than that of the neat spirulina, significant strengthening and toughening are conferred by the presence of BC sheets (Figure 4f,g). Specifically, the BC nanocomposite has an average toughness of 1.4 ± 0.2 MJ m^{-3}, which is 15× higher than the pure, untreated spirulina processed at the same conditions, while the strength reaches values as high as 42.25 ± 9.06 MPa, 98.5% higher than pure spirulina. The SEM image of the fracture surface shown in Figure 4e reveals that failure occurs at the interface between the algal matrix and the cellulose sheets, suggesting that the bonding between cellulose and algae is weaker than the matrix or the cellulose itself. Still, the positive impact of the BC sheet addition on the mechanical properties is evident, and future work could further improve composite performance by improving the interfacial interactions.

As an alternative strategy to improve the toughness and flexibility of our bioplastics and expand their processability from compression molding to extrusion, we examined the use of plasticizers. Previous literature reports that glycerol can effectively plasticize spirulina, allowing it to be processed in an extruder.[36] However, the reported mechanical properties are lower than the ones achieved in our work. In the absence of plasticizer, their pure microalgae samples attain strengths in the range of 2–6 MPa (compared to our maximum strength of unprocessed hot-pressed spirulina of 26 MPa), while in the presence of 25% glycerol, they report strengths between 1 and 2 MPa (we report strength 4–10 MPa for hot-pressed spirulina in the presence of plasticizer). Given our observations that higher temperatures and pressures are required for the transformation of spirulina to a fully bonded matrix, we chose to use sorbitol, another polyol derived from biomass, as a plasticizer instead of glycerol, due to its higher melting point and solid form at room temperature that allows easy blending with the spirulina powder. We prepared composites with 0–30 wt.% sorbitol and pressed them to 80 °C at 2 kN. The hot pressing conditions were limited by the low melting temperature of sorbitol (90 °C) and the tendency for the composites to melt and flow out of the mold. The concentration of sorbitol was kept at or below 30% for the same reason. As discussed in the previous section, the pure spirulina processed using these mild conditions has an un-bonded, packed-powder morphology, with little strength or toughness as shown in **Figure 5**c. As sorbitol concentration increases, a gradual increase in strength and toughness is observed. The 5 and 10 wt.% sorbitol bioplastics have a 41.4% and 90.5% increased modulus, 45.9% and 136.4% increased strength, and 100% and 300% increased toughness compared to the neat spirulina, as shown in Figure 5d,e. At 30 wt.% sorbitol, the strength reaches 10.2 ± 1.6 MPa and the toughness is 0.16 ± 0.05 MJ m^{-3}, marking increases of 3 and 16 times, respectively, compared to the pure spirulina control. The highest strain-to-break values (2.8%) are achieved at the maximum sorbitol concentration of 30 wt.%, showing a 2.4-fold increase over the pure spirulina. Figure 5b further demonstrates that the substantial increase in the extensibility of the bioplastics produced using the maximum sorbitol content allows an extruded filament to bend much more than the control material. Based on our mechanical tests, we conclude that the introduction of sorbitol at concentrations up to 30 wt.% promotes larger deformation prior to failure and improves the strength and toughness of spirulina.

The SEM images in Figure 5c reveal the effects of sorbitol on the micromorphology of the bioplastics. The spirulina sample with no sorbitol is comprised of weakly-bonded, intact, packed spirulina cells, as discussed previously. When sorbitol is introduced in the formulation, it melts and forms a cohesive matrix surrounding the cells, which are ultimately bonded together without being disrupted. Our imaging and mechanical results collectively suggest that intact spirulina cells can be efficiently bonded through the surrounding sorbitol matrix, which drives significant improvements in the strength, extensibility, and toughness of the bioplastics.

Ultimately, our results suggest that spirulina cells can act as a base polymer matrix with properties that can be tuned substantially by modulating the processing conditions or introducing additives, demonstrating the versatility of this material to be used in a wide variety of applications. Spirulina bioplastics are also processable using methods similar to conventional plastics, such as extrusion and compression molding, and possess other desirable properties such as compostability in soil, as discussed next.

2.3. Spirulina Bioplastics Compared to Commodity Plastics

Having characterized the mechanical properties of spirulina bioplastics and their enhancement using conventional polymer processing methods, we now compare and contrast our bioplastics with common plastics. Specifically, we focus on mechanical performance, flammability, ability to be patterned, recyclability, and compostability.

In **Figure 6**a, we present the mechanical property space of spirulina-based bioplastics covered by the discussed approaches. Elastic moduli between $E = 0.4$ and 5.3 GPa and flexural strengths from $\sigma = 1.17$ to 57.16 MPa place our bioplastics within the performance space of commodity plastics. As discussed above, our bioplastics have similar mechanical properties to PLA and drastically outperform previously reported results for bioplastics made

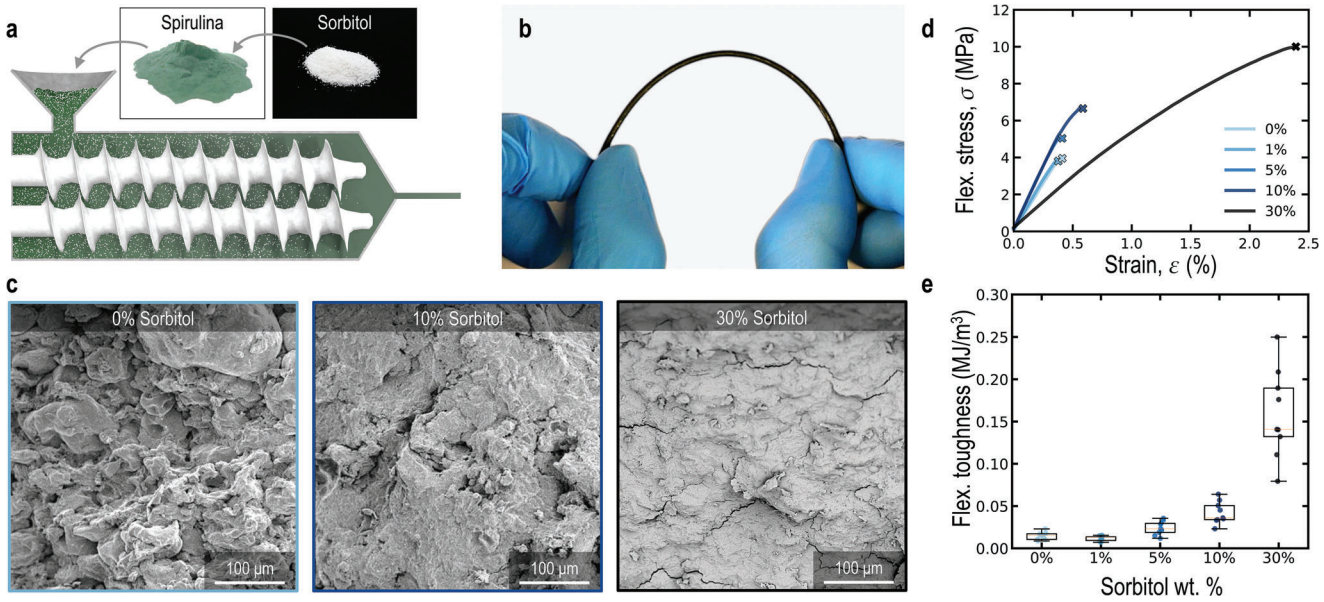

Figure 5. Sorbitol as a plasticizer for spirulina. a) Schematic for the processability of spirulina/sorbitol mixtures in a twin-screw extruder. b) Extruded filament containing 30 wt.% sorbitol demonstrating flexibility. c) SEM fracture surface images revealing the micromorphology of the spirulina bioplastics containing 0%, 10%, and 30% sorbitol. d) Representative stress-strain curves and e) boxplots for flexural toughness of the spirulina/sorbitol bioplastics.

from entire microalgae cells[36] and TPS. In the family of the biodegradable and bio-sourced PHAs and their copolymers such as poly(hydroxybutyrate-co-hydroxyvalerate) (PHBV) also shows promising properties. Neat PHBV typically has an elastic modulus around 1 GPa and strength below 20 MPa.[58] It should however be emphasized that, while showing encouraging results, PHA extraction involves complex processes that currently jeopardize its industrial scalability and limits its sustainability.[13,17,58] Thermoplastic starch provides the advantage of being biodegradable and requires low-complexity extraction methods, but its elastic modulus and strengths are typically low compared to other plastics, with $E = 0.003–1$ GPa and $\sigma = 0.2–6$.[19] Finally, while

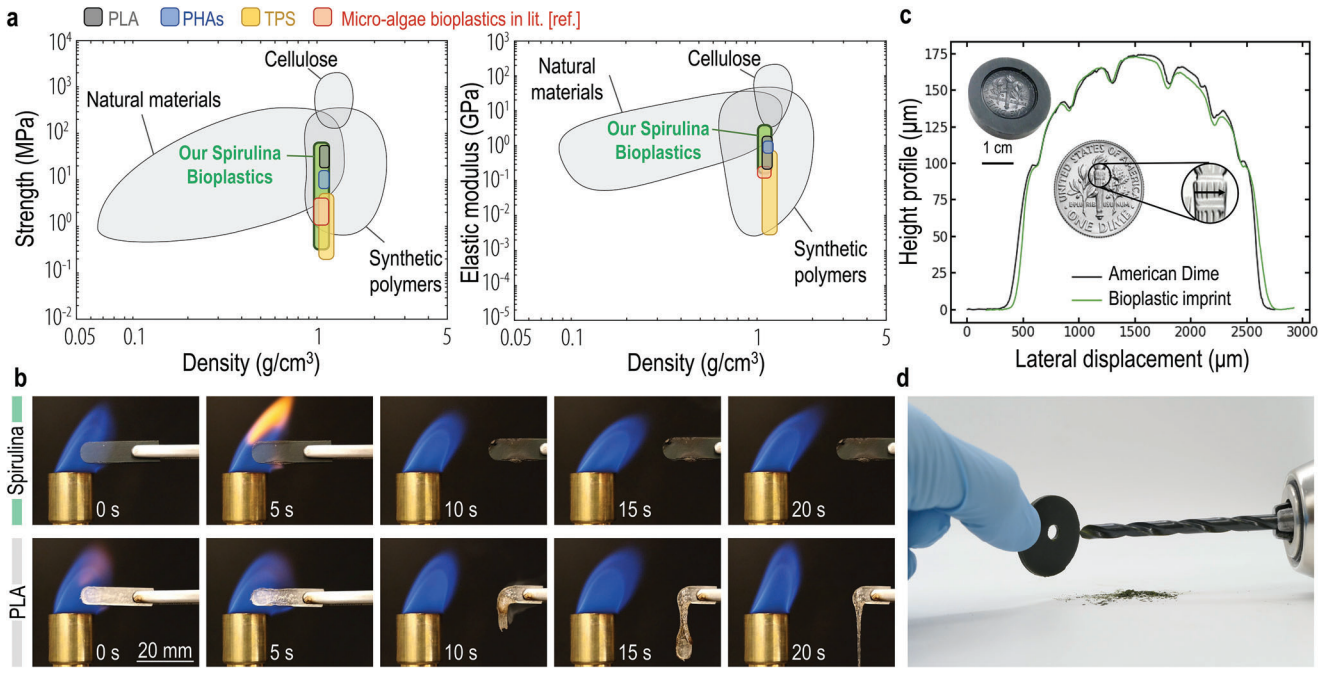

Figure 6. Spirulina in the context of commodity plastics. a) Ashby plots comparing the strength and moduli of the reported bioplastics with natural materials, synthetic plastics, and PLA. b) Flammability comparison of spirulina versus PLA. c) Contact profilometry of a portion of a dime and that same portion imprinted on a spirulina bioplastic. d) Machinability of spirulina bioplastics demonstrated using an electric drill.

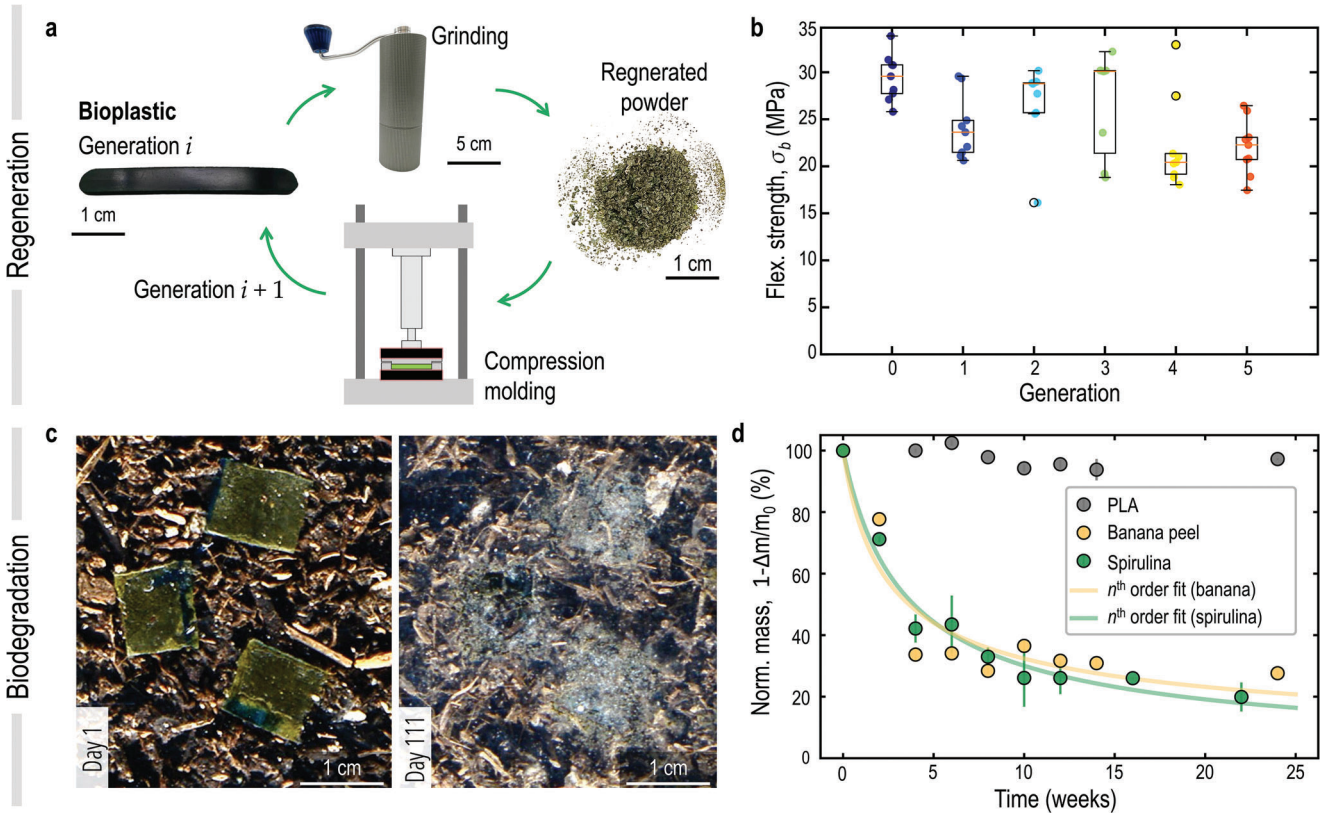

Figure 7. End of life options for spirulina bioplastics. a) Spirulina bioplastics can be recycled by grinding and re-pressing. b) Flexural strength values for regenerated spirulina samples. c) Photographs of the biodegradation of spirulina bioplastics in soil. d) Mass loss plot comparing the biodegradation of spirulina bioplastics in soil against banana peel as a positive control and PLA as a negative control.

some high-performance petroleum-derived polymers undoubtedly have more attractive mechanical properties, our bioplastics perform similarly to most consumer-based plastics such as polyethylene (PE: $E = 0.25–1.25$ GPa, $\sigma = 10–32$ MPa), polypropylene (PP: $E \approx 2$ GPa, $\sigma \approx 26$ MPa), polystyrene (PS: $E \approx 3$ GPa, $\sigma \approx 34$ MPa), or Polyethylene terephthalate (PET: $E \approx 2.3$ GPa, $\sigma \approx 55$ MPa).[59]

In terms of flammability, our bioplastics outperform the benchmark industrially compostable bioplastic, PLA, as shown in Figure 6b. After exposure to an open flame for 10 s, the spirulina bioplastic sample self-extinguished within less than 1 s and produced a char, while PLA combusted and melted leaving no solid residue.

In Figure 6c, we demonstrate that the plasticity of the spirulina bioplastics upon hot-pressing allows them to faithfully inherit imprints from positive molds. Nesting an American dime within a cylindrical mold filled with spirulina powder and subjecting it to hot pressing enabled successful transfer of the coin's design as an imprint on the spirulina surface. The surface profilometry results comparing the pattern of the coin and the imprint on the bioplastic surface show accurate patterning. The profilometer tip was run horizontally along the torch on the dime and the imprint on the spirulina, with the two curves having a root-mean-square deviation of 7.8 µm. Further evidence for the workability of the bioplastics is presented in Figure 6d where basic machining is demonstrated using conventional tooling (a hand-held drill). These abilities suggest that as manufacturing with non-traditional materials becomes more commonplace, spirulina and other similar biological matter feedstocks will be promising candidates as biodegradable polymers for commodity products.

2.4. End-of-Life Strategies

In this section, we present results on the mechanical recyclability and soil compostability of the pure spirulina bioplastics. Aiming to determine the ability of the bioplastics to be re-used and re-formed, we mechanically disintegrated a self-bonded pure spirulina bioplastic through grinding to produce a powder. The powder was subsequently incubated in ambient conditions for 24 h before re-pressing it at the same hot-pressing conditions. The flexural strength of the regenerated bioplastics is compared to the original strength (generation 0) in **Figure 7**a, showing gradual loss in strength over the course of six generations (starting at a strength of 29.5 ± 2.4 MPa at generation 0, down to 22.2 ± 4.6 MPa at generation 5). The stiffness remained consistent through the regeneration cycles, ranging from 3.5 ± 0.7 to 3.2 ± 0.5 GPa at the fourth regeneration. We note that a reduction in the mechanical properties due to thermo-oxidative and thermo-mechanical degradation is also seen in synthetic recyclable thermoplastics like polyolefins and polyesters, which rely on the introduction of stabilizers and additives to ensure

performance recovery after successive reprocessing cycles.[60] Overall, the noteworthy thermoplastic behavior and recyclability of our bioplastics suggest their applicability in areas where conventional thermoplastics are currently used.

Given that the vast majority of conventional plastic waste resides in the environment or accumulates in landfills,[3] a desirable end-of-life for our spirulina bioplastics is fast biodegradation. More specifically, the possibility for these bioplastics to degrade in soil (in a natural, aerobic environment) without the need for special conditions, such as those required for the industrial degradation of PLA, would enable end-of-life disposal in natural environments with minimal environmental impact. In Figure 7c, we present photographs of spirulina samples buried in soil for natural decomposition right after burying (day 1), and after approximately 16 weeks (111 days). The advanced biodegradation is visually observed from the blending in of the samples with soil on day 111.

To quantitatively assess this degradation rate, we measured the mass loss over time of spirulina bioplastics buried in soil, as compared to a positive control (banana peels) and a negative control (PLA). As reported in Figure 7d, the spirulina bioplastics degrade at a rate comparable to the positive control, with a rapid mass loss upon exposure to soil. Indeed, during the first 5 weeks of incubation in soil, both the positive control and our bioplastics lose approximately 60% of their dry mass and subsequently continue to slowly degrade. A mass loss of about 80% is achieved after 22 weeks, both for the bioplastics and the positive control. This type of decelerating degradation has been observed in many types of biodegradation tests (enzymatic, in water, in soil) for various biomass materials.[61] Considering that decelerating degradation kinetics are often well described by reaction order models,[62,63] we found that an n^{th} order reaction model of the type:

$$\frac{\mathrm{d}\alpha}{\mathrm{d}t} = k(1-\alpha)^n, \tag{2}$$

where $\alpha = \Delta m/m_0$ corresponds to the degree of conversion with Δm the mass variation and m_0 the initial mass of the buried sample, gives a reasonable fit of our data. A least-square fitting provided values of $n = 2.89$, $k = 0.29$ and $n = 2.28$, $k = 0.39$ for banana and spirulina, respectively, with corresponding root-mean-square error values of 0.013 and 0.028. To the best of the authors' knowledge, no prior investigation has focused on the degradation kinetics of spirulina in soil. One study reported a satisfactory first-order model ($n = 1$) for the anaerobic biodegradation of spirulina in the presence of sewage sludge,[64] but additional investigations will be necessary to further shine light on the soil-degradation reactions and kinetics of our bioplastics. Still, our results reveal the natural biodegradation capability of the spirulina bioplastics over the course of a few weeks.

Finally, analyzing the environmental impacts associated with the manufacturing process of the spirulina bioplastics offers valuable insights into the true potential of the suggested bioplastics class. Assuming that the environmental impact associated with hot-pressing spirulina powder into a functional part is similar to the impact of the molding step required to fabricate a part from traditional plastic pellets, we restrict our comparison to the cradle-to-factory-gate production of spirulina powder versus traditional plastic pellets. Given that the growth of plants or algae takes up carbon from the atmosphere, their use as feedstocks in bioplastics enables the fabrication of carbon-neutral or carbon-negative materials. Upon growth, microalgae capture around 1.8 kg CO_2 per kg of dry biomass,[65] providing an attractive advantage over fuel-derived polymers. It should be noted that the CO_2 emissions associated with fertilizers, heating, pumping, harvesting, and drying are highly dependent on the installations and therefore vary significantly across sources. By using the global warming potential (GWP) values of the production of wet spirulina[65] and the drying process of microalgae,[66] we estimate a GWP of -0.54 kg CO_2 per kg for our dry spirulina powder. While it is important to note that Tzachor et. al's production method is not typical, it is an indication that newer and cleaner methods of microalgae production are possible. In a recent study by Beckstrom et al., the authors reported an overall net carbon credit of -0.315 kg CO_2 per kg of dry microalgae in their best-case models.[66] For comparison, the GWP of 1 kg of high-density polyethylene pellets was reported to be 1.9 kg CO_2 by PlasticsEurope,[67] while polypropylene was reported to have a GWP of 2.0 kg CO_2. In 2019, a cradle-to-gate study[68] showed the GWP of Corbion PLA pellets to be 0.501 kg CO_2 per kg of PLA. The potential negative GWP of the spirulina bioplastics, their ability to be processed using conventional polymer manufacturing infrastructure, their impressive attainable mechanical properties, and their end-of-life fates, suggest that this material class represents a viable alternative to commodity plastics for a wide range of applications.

3. Conclusion

The design and fabrication of environmentally friendly materials must be investigated to mitigate the plastic pollution generated by non-degradable polymers. In this article, we have successfully demonstrated the production of bulk, thermoformable plastics using an abundant, photosynthetic microorganism, spirulina. This wasteless transformation does not require additional binders or solvents and yields bioplastics with mechanical properties comparable to polystyrene (34 MPa tensile strength, 3 GPa flexural modulus, 1.6% elongation to break). We have shown further control of the mechanical properties by preprocessing the biomass through sonication and by introducing fillers, which allow us to expand the attainable bending strength by 124 %, the modulus by 71 % and the toughness by 900 %. We have reported the first step toward understanding the chemical transformations driving the macroscopic bonding upon hot-pressing, though further investigations will be required to elucidate the precise reaction mechanisms. These algae-based bioplastics are machinable and have remarkable shape fidelity when making imprints. They also show potential to be used as flame-safe materials as they self-extinguish and char almost immediately after exposure to an open flame. These bioplastics can be given a second life by grinding into powder for re-processing, or they can harmlessly return to the environment by degrading in soil. Given these attractive properties and the fact that spirulina is carbon negative, the proposed material family is appealing for packaging or consumer good applications, which are currently mostly unsustainably sourced by petroleum-derived polymers.

4. Experimental Section

Materials: Organic spirulina was purchased from Nuts.com. Sorbitol and MMT nanoplatelets were purchased from Sigma–Aldrich, USA. Bacterial cellulose was produced from a kombucha culture as reported in Ref. [23]

Fabrication of Bioplastics: An Analog Vortex Mixer from VWR was used for initial powder mixing. The premixed powders were then subjected to a compression molding process on a TMAX-SYP-600 hot press from TMAXCN, using custom-made stainless steel molds. These molds were loaded with 1 g of spirulina per sample to produce beams with lengths and widths of approximately 60 and 8 mm, respectively. Samples were curved at the ends with radii of approximately 3.5 mm. To examine the effects of temperature and pressure on the pure bioplastics, temperatures ranged from 60 to 160 °C by steps of 20 °C, while pressing forces of 2, 7, 20, and 35 kN were used. Conversions to pressure on the powder are available in Table S1 (Supporting Information). The duration of the hot-pressing process was measured starting when pressing force was achieved. The samples that were tested in compression had a cube geometry (length of 25.4 mm for each side), and were prepared using an aluminum square tube with an inner edge length of 1 inch. The hot press conditions for those samples were set to 140 °C, 7 kN, and 10 min, although extra time was allowed for packing the powder down in steps to avoid exceeding the stroke of the hot press piston.

For the bioplastics from dissociated spirulina, an aqueous suspension of the as-received cells in a 1:10 w/w concentration was sonicated for 20 min using Fisher Scientific Model 505 probe sonicator, on an ice bath. After sonication, the dissociated biomatter suspension was freeze-dried using a Freezone lyophilizer from Labcono Corp. For the spirulina/nanoclay composites, the pre-sonicated and freeze-dried dissociated spirulina powder was mixed with the nanoclay powder at the desired concentrations prior to being hot-pressed. To produce spirulina/BC composites, BC sheets with dimensions of 40 mm by 1 mm were laid along the *X–Y* plane of the mold, in between pure spirulina powder, creating a layered structure that was hot pressed at 140 °C/7 kN. The BC sheets made up 10 wt.% of the biocomposite. To prepare the spirulina/sorbitol biocomposites, the premixed powders at the desired concentrations of 1, 5, 10, and 30 wt.% in sorbitol, were first compounded on a Scientific Process 11 Twin-Screw Extruder from Thermo Fisher, operating at 40 rpm, with a uniform temperature profile of 90 °C, before being hot pressed at 80 °C and 7 kN, for 1 min.

Characterization–Mechanical Testing: Three-point bend specimens were desiccated for 24 h at 23 °C, before being tested on an AGS-X test frame from Shimadzu Scientific Instruments. A minimum of nine samples were tested for each composition at a 0.5% per second strain rate and 40 mm gauge length. Compression testing was performed using an Instron 4505 universal test frame with a 5500R upgrade. A 100 kN load cell was used. A minimum of five samples per testing direction were tested at 0.5% per second strain rate.

Characterization–Scanning Electron Microscopy: Scanning electron microscopy (SEM) was conducted on an Apreo VP from ThermoFisher Scientific, on samples previously sputter coated with 4 nm of platinum on an EM ACE600, produced by Leica Microsystems.

Characterization–Fourier Transform Infrared Spectroscopy: Fourier transform infrared spectroscopy (FTIR) was performed using a Thermo Scientific Nicolet iS10 FTIR in ATR mode. Spectra were obtained with a resolution of 2 cm^{-1} and 128 scans. Scans were performed between 400 and 4000 cm^{-1}. Spectra were vector normalized and distributed vertically for ease of comparison. Peak identification was performed using the scipy.signal.find_peaks function in Python.

Characterization–X-Ray Photoelectron Spectroscopy: All X-ray photoelectron spectroscopy (XPS) spectra were taken on a Kratos Axis-Ultra DLD spectrometer. This instrument has a monochromatized Al Kα X-ray and a low energy electron flood gun for charge neutralization. X-ray spot size for these acquisitions was on the order of 700 × 300 µm. Pressure in the analytical chamber during spectral acquisition was less than 5×10^{-9} Torr. Pass energy for survey and detailed spectra (composition) was 80 eV. Pass energy for the high resolution spectra was 20 eV. The take-off angle (the angle between the sample normal and the input axis of the energy analyzer) was 0 ° (0 degree take-off angle 100 Å sampling depth). CasaXPS was used to peak fit the high resolution spectra. For the high-resolution spectra, a Shirley background was used and all binding energies were referenced to the C 1s C–C bonds at 285.0 eV.

Characterization–Elemental Analysis and Calculation of Protein Content: The concentration of carbon and nitrogen in spirulina powder was assessed using a CHN Analyzer 2400 Model from PerkinElmer operating in combustion mode at 925 °C. The protein content of spirulina can be calculated qualitatively as the product of the nitrogen content and an indirect conversion factor. The factor used most commonly was 6.25, however, quantitative measurements of protein content indicate that the use of this factor may result in overestimation of the protein content of most algae. In fact, Angell et al. propose that five may be a more accurate conversion factor for seaweeds.[69] To take into account the uncertainty of qualitative, indirect conversion from nitrogen content, we present the protein content as a range of compositions calculated using both customary and conservative conversion factors.

Characterization–Thermal Analysis: Thermogravimetric analysis (TGA) was performed on a Discovery TGA 550, from TA Instruments. Samples of 13 ± 4 mg of each material were subjected to heating from room temperature to 1000 °C at a heating rate of 10 °C min^{-1} in a nitrogen gas flow of 25µL min^{-1}. Differential Scanning Calorimetry (DSC) was done on a Discovery 2500 DSC from TA Instruments, in hermetically sealed TZero aluminum pans. Each specimen went through two heating and cooling cycles each, at rates of 10 °C min^{-1}, with isothermal holds of 1 min between each cycle, from -75 to 200 °C.

Characterization–Profilometry: Optical profilometry was conducted using an Olympus OLS4100, from Olympus IMS at a 20X objective. Contact profilometry was conducted using a Bruker DektakXT, from Bruker in Billerica, MA, USA.

Characterization–Biodegradation: The soil biodegradation study was performed by burying a total of 36 samples with dimensions 5 × 5 × 1 mm^3 of each material in gardening soil which was regularly watered to keep wet. At every time step, a set of four samples was recovered to measure their mass loss after cleaning them in deionized water and drying them in an oven (60 °C), for 48 h to obtain the dry weight.

Supporting Information

Supporting Information is available from the Wiley Online Library or from the author.

Acknowledgements

The authors acknowledge financial support in the form of gift funds from Microsoft Research and Meta Platforms, Inc. I.R.C. acknowledges funding from the National Science Foundation Graduate Research Fellowship under Grant No. DGE-2140004. Part of this work was conducted at the Molecular Analysis Facility, a National Nanotechnology Coordinated Infrastructure (NNCI) site at the University of Washington, which is supported in part by funds from the National Science Foundation (awards NNCI-2025489, NNCI-1542101), the Molecular Engineering & Sciences Institute, and the Clean Energy Institute.

Conflict of Interest

The authors declare no conflict of interest.

Data Availability Statement

The data that support the findings of this study are available from the corresponding author upon reasonable request.

Keywords

biodegradation, bioplastics, recycling, spirulina

Received: February 21, 2023
Revised: May 6, 2023
Published online:

[1] I. Campbell, M.-Y. Lin, H. Iyer, M. Parker, J. Fredricks, K. Liao, A. Jimenez, P. Grandgeorge, E. Roumeli, *Annu. Rev. Mater. Res.* **2023**, *53*.
[2] A. K. Mohanty, S. Vivekanandhan, J.-M. Pin, M. Misra, *Science* **2018**, *362*, 536.
[3] T. H. Epps, III, L. T. J. Korley, T. Yan, K. L. Beers, T. M. Burt, *JACS Au* **2022**, *2*, 3.
[4] D. K. Schneiderman, M. A. Hillmyer, *Macromolecules* **2017**, *50*, 3733.
[5] C. M. Rochman, M. A. Browne, B. S. Halpern, B. T. Hentschel, E. Hoh, H. K. Karapanagioti, L. M. Rios-Mendoza, H. Takada, S. Teh, R. C. Thompson, *Nature* **2013**, *494*, 169.
[6] X. Zhang, M. Fevre, G. O. Jones, R. M. Waymouth, *Chem. Rev.* **2018**, *118*, 839.
[7] H. A. Leslie, M. J. M. van Velzen, S. H. Brandsma, A. D. Vethaak, J. J. Garcia-Vallejo, M. H. Lamoree, *Environ. Int.* **2022**, *163*, 107199.
[8] A. A. Lacis, G. A. Schmidt, D. Rind, R. A. Ruedy, *Science* **2010**, *330*, 356.
[9] K. J. Jem, B. Tan, *Adv. Ind. Eng. Polym. Res.* **2020**, *3*, 60.
[10] M. A. Hillmyer, W. B. Tolman, *Acc. Chem. Res.* **2014**, *47*, 2390.
[11] F. M. Haque, J. S. A. Ishibashi, C. A. L. Lidston, H. Shao, F. S. Bates, A. B. Chang, G. W. Coates, C. J. Cramer, P. J. Dauenhauer, W. R. Dichtel, C. J. Ellison, E. A. Gormong, L. S. Hamachi, T. R. Hoye, M. Jin, J. A. Kalow, H. J. Kim, G. Kumar, C. J. LaSalle, S. Liffland, B. M. Lipinski, Y. Pang, R. Parveen, X. Peng, Y. Popowski, E. A. Prebihalo, Y. Reddi, T. M. Reineke, D. T. Sheppard, J. L. Swartz, et al., *Chem. Rev.* **2022**, *122*, 6322.
[12] J. M. Bolton, M. A. Hillmyer, T. R. Hoye, *ACS Macro Lett.* **2014**, *3*, 717.
[13] Y. F. Tsang, V. Kumar, P. Samadar, Y. Yang, J. Lee, Y. S. Ok, H. Song, K.-H. Kim, E. E. Kwon, Y. J. Jeon, *Environ. Int.* **2019**, *127*, 625.
[14] K. Roja, D. Ruben Sudhakar, S. Anto, T. Mathimani, *Biocatal. Agric. Biotechnol.* **2019**, *22*, 101358.
[15] S. S. Costa, A. L. Miranda, D. d. J. Assis, C. O. Souza, M. G. de Morais, J. A. V. Costa, J. I. Druzian, *Algal Res.* **2018**, *33*, 231.
[16] E. Bugnicourt, P. Cinelli, A. Lazzeri, V. Alvarez, *Express Polym. Lett.* **2014**, *8*, 791.
[17] M. Koller, L. Maršálek, M. M. de Sousa Dias, G. Braunegg, *New Biotechnol.* **2017**, *37*, 24.
[18] K. M. Dang, R. Yoksan, E. Pollet, L. Avérous, *Carbohydr. Polym.* **2020**, *242*, 116392.
[19] Y. Zhang, C. Rempel, Q. Liu, *Crit. Rev. Food Sci. Nutr.* **2014**, *54*, 1353.
[20] L. Avérous, P. J. Halley, *Biofuels Bioprod. Biorefin.* **2009**, *3*, 329.
[21] R. J. Moon, A. Martini, J. Nairn, J. Simonsen, J. Youngblood, *Chem. Soc. Rev.* **2011**, *40*, 3941.
[22] Q. Xia, C. Chen, Y. Yao, J. Li, S. He, Y. Zhou, T. Li, X. Pan, Y. Yao, L. Hu, *Nat. Sustainability* **2021**, *4*, 627.
[23] J. L. Fredricks, M. Parker, P. Grandgeorge, A. M. Jimenez, E. Law, M. Nelsen, E. Roumeli, *MRS Commun.* **2022**, *12*, 394.
[24] J. L. Fredricks, A. M. Jimenez, P. Grandgeorge, R. Meidl, E. Law, J. Fan, E. Roumeli, *J. Polym Sci.* **2023**.
[25] G. Tedeschi, S. Guzman-Puyol, L. Ceseracciu, U. C. Paul, P. Picone, M. Di Carlo, A. Athanassiou, J. A. Heredia-Guerrero, *Biomacromolecules* **2020**, *21*, 910.
[26] K. Sakakibara, Y. Moriki, Y. Tsujii, *ACS Appl. Polym. Mater.* **2019**, *1*, 178.
[27] A. J. Onyianta, D. O'Rourke, D. Sun, C.-M. Popescu, M. Dorris, *Cellulose* **2020**, *27*, 7997.
[28] C. Mathiot, P. Ponge, B. Gallard, J.-F. Sassi, F. Delrue, N. Le Moigne, *Carbohydr. Polym.* **2019**, *208*, 142.
[29] C. Zhang, P.-L. Show, S.-H. Ho, *Bioresour. Technol.* **2019**, *289*, 121700.
[30] J. L. Fredricks, H. Iyer, R. McDonald, J. Hsu, A. M. Jimenez, E. Roumeli, *J. Polym. Sci.* **2021**, *59*, 2878.
[31] E. Roumeli, R. Hendrickx, L. Bonanomi, A. Vashisth, K. Rinaldi, C. Daraio, *PNAS* **2022**, *119*, 15.
[32] A. Manjula-Basavanna, A. M. Duraj-Thatte, N. S. Joshi, *Adv. Funct. Mater.* **2021**, *31*, 2010784.
[33] A. M. Duraj-Thatte, A. Manjula-Basavanna, N.-M. D. Courchesne, G. I. Cannici, A. Sánchez-Ferrer, B. P. Frank, L. van't Hag, S. K. Cotts, D. H. Fairbrother, R. Mezzenga, N. S. Joshi, *Nat. Chem. Biol.* **2021**, *17*, 732.
[34] M. Haneef, L. Ceseracciu, C. Canale, I. S. Bayer, J. A. Heredia-Guerrero, A. Athanassiou, *Sci. Rep.* **2017**, *7*, 41292.
[35] W. Sun, M. Tajvidi, C. G. Hunt, G. McIntyre, D. J. Gardner, *Sci. Rep.* **2019**, *9*, 13766.
[36] M. A. Zeller, R. Hunt, A. Jones, S. Sharma, *J. Appl. Polym. Sci.* **2013**, *130*, 3263.
[37] A. Z. Naser, I. Deiab, B. M. Darras, *RSC Adv.* **2021**, *11*, 17151.
[38] D. M. Byler, H. Susi, *Biopolymers* **1986**, *25*, 469.
[39] S. Cai, B. R. Singh, *Bioph. Chem.* **1999**, *80*, 7.
[40] G. Anderle, R. Mendelsohn, *Bioph. J.* **1987**, *52*, 69.
[41] S. Keten, Z. Xu, B. Ihle, M. J. Buehler, *Nat. Mater.* **2010**, *9*, 359.
[42] S. Xiao, S. Xiao, F. Gräter, *Phys. Chem. Chem. Phys.* **2013**, *15*, 8765.
[43] S. Cichosz, A. Masek, *Materials* **2020**, *13*, 4573.
[44] T. Lafarga, J. M. Fernández-Sevilla, C. González-López, F. G. Acién-Fernández, *Food Res. Int.* **2020**, *137*, 109356.
[45] D. G. Bortolini, G. M. Maciel, I. d. A. A. Fernandes, A. C. Pedro, F. T. V. Rubio, I. G. Brancod, C. W. I. Haminiuk, *Food Chem.* **2022**, *5*, 100134.
[46] M. d. Oliveira, M. Monteiro, P. Robbs, S. Leite, *Aquacult. Int.* **1999**, *7*, 261.
[47] S. Bensehaila, A. Doumandji, L. Boutekrabt, H. Manafikhi, I. Peluso, K. Bensehaila, A. Kouache, A. Bensehaila, *African J. Biotech.* **2015**, *14*, 1649.
[48] K. Kusmiyati, A. Heratri, S. Kubikazari, A. Hidayat, H. Hadiyanto, *Int. Energy J.* **2020**, *20*, 611.
[49] M.-H. Jau, S.-P. Yew, P. S. Toh, A. S. Chong, W.-L. Chu, S.-M. Phang, N. Najimudin, K. Sudesh, *Int. J. Biol. Macromol.* **2005**, *36*, 144.
[50] B. L. Tardy, B. D. Mattos, C. G. Otoni, M. Beaumont, J. Majoinen, T. Kämäräinen, O. J. Rojas, *Chem. Rev.* **2021**, *121*, 14088.
[51] P. S. Corrêa, C. M. L. L. Teixeira, *J. Appl. Phycol.* **2021**, *33*, 1487.
[52] R. R. Retamal Marín, F. Babick, M. Stintz, *Powder Technol.* **2017**, *318*, 451.
[53] S. R. Chia, K. W. Chew, H. Y. Leong, S. Manickam, P. L. Show, T. H. P. Nguyen, *Biochem. Eng. J.* **2020**, *398*, 125613.
[54] M.-I. Chan, K.-t. Lau, T.-t. Wong, M.-p. Ho, D. Hui, *Compos. Part B* **2011**, *42*, 1708.
[55] M. Heydari-Meybodi, S. Saber-Samandari, M. Sadighi, *Compos. Sci. Technol.* **2015**, *117*, 379.
[56] F. Uddin, *Metall. Mater. Trans. A* **2008**, *39*, 2804.
[57] J. Wang, J. Tavakoli, Y. Tang, *Carbohydr. Polym.* **2019**, *219*, 63.
[58] E. Ten, L. Jiang, J. Zhang, M. P. Wolcott, *Biocomposites* **2015**, 39, ISBN 978-1-78242-373-7.
[59] T. R. Crompton, in *Physical Testing of Plastics*, Smithers Rapra, Shrewsbury, Shropshire, UK **2012**.
[60] Z. O. Schyns, M. P. Shaver, *Macromol. Rapid Commun.* **2021**, *42*, 2000415.
[61] N. B. Erdal, M. Hakkarainen, *Biomacromolecules* **2022**, *23*, 2713.
[62] S. Vyazovkin, A. K. Burnham, J. M. Criado, L. A. Pérez-Maqueda, C. Popescu, N. Sbirrazzuoli, *Thermochim. Acta* **2011**, *520*, 1.

[63] S. Vyazovkin, A. K. Burnham, L. Favergeon, N. Koga, E. Moukhina, L. A. Pérez-Maqueda, N. Sbirrazzuoli, *Thermochim. Acta* **2020**, *689*, 178597.
[64] B. Shi, C. Bunyard, D. Palfery, *Carbohydr. Polym.* **2010**, *82*, 401.
[65] A. Tzachor, A. Smidt-Jensen, A. Ramel, M. Geirsdóttir, *Mar. Biotechnol.* **2022**, *24*, 991.
[66] B. D. Beckstrom, M. H. Wilson, M. Crocker, J. C. Quinn, *Algal Res.* **2020**, *46*, 101769.
[67] M. R. Yates, C. Y. Barlow, *Resour. Conserv. Recycl.* **2013**, *78*, 54.
[68] A. Morão, F. De Bie, *J. Polym. Environ.* **2019**, *27*, 2523.
[69] A. R. Angell, L. Mata, R. de Nys, N. A. Paul, *J. Appl. Phycol.* **2016**, *28*, 511.